Impact of Insulin-Like Growth Factor Receptor-I Function on Angiogenesis, Growth, and Metastasis of Colon Cancer

Niels Reinmuth, Fan Fan, Wenbiao Liu, Alexander A. Parikh, Oliver Stoeltzing, Young D. Jung, Corazon D. Bucana, Robert Radinsky, Gary E. Gallick, and Lee M. Ellis

Departments of Cancer Biology (NR, FF, WL, AAP, OS, YDJ, CDB, RR, GEG, LME) and Surgical Oncology (LME), The University of Texas M. D. Anderson Cancer Center, Houston, Texas

SUMMARY: Insulin-like growth factors and their principal receptor, IGF-I receptor (IGF-IR), are frequently expressed in human colon cancers and play a role in preventing apoptosis, enhancing cell proliferation, and inducing expression of vascular endothelial growth factor (VEGF). The role of IGF-IR in regulating angiogenesis and metastases of human colon cancer has not been elucidated. To determine the in vitro and in vivo effects of IGF-IR in human colon cancer growth and angiogenesis, human KM12L4 colon cancer cells were transfected with a truncated dominant-negative form of IGF-IR (IGF-IR dom-neg). IGF-IR dom-neg–transfected cells demonstrated markedly decreased constitutive expression of VEGF mRNA and protein. Subcutaneous injections of IGF-IR dom-neg–transfected cells in nude mice led to significantly decreased tumor growth ($p < 0.05$) that was associated with decreased tumor cell proliferation, VEGF expression, and vessel count and with increased tumor cell apoptosis ($p < 0.05$ for all parameters compared with controls). In addition, pericyte coverage of endothelial cells was significantly decreased in tumors from IGF-IR dom-neg–transfected cells. Following this observation, we demonstrated in vitro that vascular smooth muscle cells migrated significantly less in conditioned medium derived from IGF-IR dom-neg–transfected cells compared with medium from control cells. After splenic injections, IGF-IR dom-neg transfectants failed to produce liver metastases, in contrast to parental cells and mock transfectants ($p < 0.05$). In addition, IGF-IR dom-neg–transfected cells failed to form liver tumors after direct injection into the liver. These studies demonstrate that the IGF-IR plays an important role in multiple mechanisms that mediate the growth, angiogenesis, and metastasis of human colon cancer. IGF-IR is a valid target for the therapy of human colon cancer. (*Lab Invest 2002, 82:1377–1389*).

A variety of tumor systems including colon cancers demonstrate altered expression of insulin-like growth factor-I and -II (IGF-I, -II) and their principal receptor, IGF-I receptor (IGF-IR). Colorectal carcinomas have 10 to 50 times higher levels of IGF-I and -II compared with adjacent uninvolved colonic mucosa (Freier et al, 1999; Hakam et al, 1999; Michell et al, 1997). The source of the most IGF-I is the liver, the most frequent site of metastasis from colon cancer.

The IGF-IR, a tyrosine kinase receptor, consists of two α and two β subunits (Baserga et al, 1997a). The α subunits are entirely extracellular chains, containing a cysteine-rich domain responsible for ligand binding

(Baserga et al, 1997a; Werner and Le Roith, 1997). The β subunits display a highly hydrophobic transmembrane domain, which divides the β subunit into an extracellular and an intracellular region containing a tyrosine kinase domain (Baserga et al, 1997a; Werner and Le Roith, 1997). Several authors have demonstrated that the IGF-IR is crucial for maintaining normal growth and development (Liu et al, 1993; Werner and Le Roith, 1997). For example, homozygous IGF-IR knockout mice exhibit severe growth deficiency and invariably die at birth (Liu et al, 1993). Upon activation, the IGF-IR stimulates synthesis of RNA and DNA, cell proliferation, differentiation, and survival (Baserga et al, 1997a; Rubin and Baserga, 1995; Werner and Le Roith, 1997). When activated above a certain threshold, IGF-IR leads to growth in serum-free medium and to the establishment of a transformed phenotype (Baserga et al, 1997b). In addition, a minimal level of IGF-IR seems to be required for tumor growth and survival (Butler et al, 1998).

In human colon cancer cells, IGF-IR not only is present but is frequently overexpressed (Freier et al, 1999; Hakam et al, 1999). However, the biologic importance of IGF-IR in colon cancer has not been elucidated. In addition to the known functions of

IGF-IR, it also might be involved in tumor angiogenesis. As recently demonstrated, IGF-I induces the expression of the vascular endothelial growth factor (VEGF), likely through the IGF-IR (Akagi et al, 1998; Warren et al, 1996; Wu et al, 2002; and YD Jung and LM Ellis, unpublished data, 2001). VEGF is a fundamental regulator of angiogenesis and exists as several isoforms owing to alternate splicing (121, 145, 165, 189, and 206 amino acid isoforms) (Brown et al, 1997; Warren et al, 1996). Growth and metastasis of tumors depend on their ability to induce the growth of new blood vessels (Ellis and Fidler, 1996; Ellis et al, 2000; Folkman, 1992), and interest in understanding the complex regulatory mechanisms of tumor angiogenesis has exploded over the past 10 years.

The role of IGF-I and IGF-IR in malignant growth is at times difficult to define because IGF-binding proteins (IGFBPs) may modulate the biologic effects of IGF (reviewed by Singh and Rubin, 1993). These factors can bind IGF-I and either enhance or inhibit its ability to bind to its receptor (depending on the specific IGFBP), thus affecting IGF-I's biologic activity. However, VEGF induction by IGF-I is most likely not affected by IGFBPs because a truncated IGF-I lacking the binding site for IGFBPs does not alter VEGF induction (Akagi et al, 1998; Singh et al, 1994).

To further our understanding of the role of the IGF-IR in human colon cancer growth, we stably transfected a human colon cancer cell line, KM12L4, with a truncated IGF-IR (IGF-IR dom-neg) lacking the cytosolic kinase domain. IGF-IR dom-neg forms a nonfunctional heterodimer with endogenous IGF-IR (Prager et al, 1992, 1994). We found that constitutive and inducible VEGF expression was strongly impaired in IGF-IR dom-neg–transfected cells. In vivo, subcutaneous growth of IGF-IR dom-neg–transfected cells in nude mice was significantly reduced, and this was associated with a decrease in proliferation, blood vessel formation, and pericyte coverage. In in vitro studies, conditioned medium from these cells impaired migration of human vascular smooth muscle cells (hVSMCs). In addition, IGF-IR dom-neg–transfected cells failed to form liver metastases or liver tumors after injection into the spleen or the liver, respectively. These results suggest that the IGF-IR plays a multifunctional role in human colon cancer growth and affects tumor angiogenesis by decreasing VEGF expression and inhibiting pericyte coverage.

Results

Characteristics of Human Colon Cancer Cells Transfected with Truncated IGF-IR

KM12L4 cells were transfected with a IGF-IR dom-neg or the empty vector (pcDNA3). Successful transfection was confirmed by nondenaturing Western blot analysis using antibodies directed against the α and β subunits of the IGF-IR. IGF-IR dom-neg–transfected cells demonstrated strong additional bands indicating the 300-kDa mutant homodimer and the 360-kDa wild-type/mutant hybrid, respectively, as described by

Prager et al (1992) (data not shown). Transfection with pcDNA3 had no gross effect on cell morphology. In contrast, IGF-IR dom-neg–transfected KM12L4 cells had a more irregular cell shape and formed colonies of greater variability in size and shape than did controls. As determined by 3-(4,5-dimethylthiazol-2-yl)-2,5-diphenyltetrazolium bromide (MTT) assay in vitro, there was a significant decrease of $\sim$35% in the growth of IGF-IR dom-neg–transfected cells compared with controls after 48 hours ($p < 0.05$, not shown).

### Constitutive and Induced Levels of VEGF in Transfected Cells

As determined by Northern blot analysis, constitutive expression of VEGF mRNA was strongly decreased in several IGF-IR dom-neg–transfected clones (Fig. 1A). In sharp contrast, parental and mock-transfected cells demonstrated high constitutive VEGF expression. Even though IGF-IR dom-neg–transfected cells showed some induction of VEGF in response to IGF-I, this induction was less than 25% of that in controls. Semiquantitative RT-PCR demonstrated that all isoforms of VEGF mRNA were decreased relatively equally in the IGF-IR dom-neg–transfected cells (not shown). The transfected clone showing the least VEGF expression was used for further experiments. Using an ELISA kit for VEGF, constitutive and IGF-I–induced VEGF protein concentrations were significantly lower in conditioned medium from IGF-IR dom-neg–transfected cells than in conditioned medium from control cells ($p < 0.001$; Fig. 1B).

Effect of Transfection with IGF-IR dom-neg on Signaling Pathways

IGF-I signaling involves multiple intracellular pathways including regulators of cell proliferation and/or survival, eg, mitogen-activated protein kinase/Erk (MAPK/Erk) and PI-3 kinase (PI-3K)/Akt pathways (Satyamoorthy et al, 2001; Solorzano et al, 2001). IGF-IR dom-neg–transfected cells demonstrated constitutively decreased phosphorylated levels of Erk1/2 and Akt as determined by Western blot analysis (Fig. 2). However, the addition of IGF-I stimulated phosphorylation of Erk1/2 and Akt in control and IGF-IR dom-neg–transfected cells, suggesting some retention of IGF-IR function (not shown).

Growth and Tumor Formation In Vivo of IGF-IR dom-neg–Transfected Cells

To study the effect of IGF-IR on tumor formation in vivo, parental, pcDNA3-transfected, and IGF-IR dom-neg–transfected KM12L4 cells were injected subcutaneously into nude mice (9–10/group). After 14 days, the mice injected with control cells (parental and pcDNA3-transfected) developed tumors that exceeded 1.2 cm in diameter, at which point all mice were killed. Mice injected with parental and pcDNA3-transfected cells formed large tumors that were similar in size (P = NS). In contrast, mice injected with IGF-IR

A

B
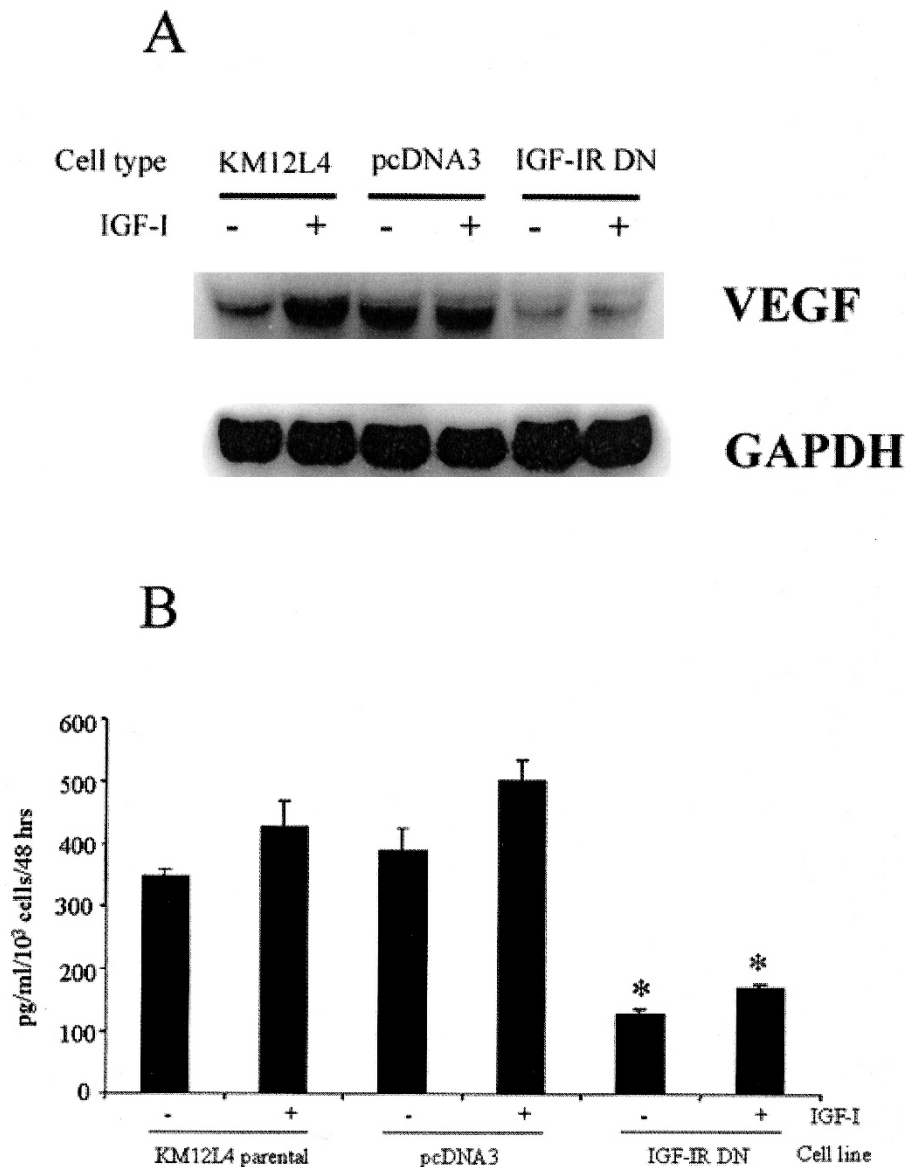
Figure 1.

Vascular endothelial growth factor (VEGF) induction by IGF-I in cells transfected with the IGF-IR dom-neg construct. A, KM12L4 cells were transfected with a truncated IGF-IR (*IGF-IR DN*) and incubated with IGF-I (100 ng/mL) for 24 hours. VEGF mRNA expression was determined by Northern blot analysis. IGF-IR dom-neg–transfected cells showed decreased constitutive and inducible VEGF mRNA levels. B, Conditioned medium was harvested from KM12L4 parental and transfected cells treated with or without IGF-I (100 ng/mL) for 48 hours, and the VEGF concentration was assessed by ELISA. IGF-IR dom-neg–transfected cells secreted significantly less VEGF protein than did control cells (parental and pcDNA3-transfected) with similar treatment (*$p < 0.001$).

dom-neg–transfected cells developed significantly smaller tumors than the other groups ($p < 0.001$) (Fig. 3A). Furthermore, tumor weight was significantly decreased by about 70% in mice injected with IGF-IR dom-neg–transfected cells compared with controls (Fig. 3B). Representative pictures are shown in Figure 4.

Growth and Metastasis Formation of IGF-IR dom-neg–Transfected Cells in the Liver

Because the liver represents the most frequent site of distant metastasis from colon cancer, we injected parental and transfected KM12L4 colon cancer cells into the spleen (9–10 mice/group) to induce the de-

velopment of liver metastases (Bruns et al, 2000a). About half of the mice injected with parental (4/9) and mock-transfected cells (5/9) developed liver metastases. In contrast, metastasis formation was not observed in the group injected with IGF-IR dom-neg–transfected cells (0/10; $p < 0.05$; χ^2 analysis) (Fig. 4). All mice developed splenic tumors; however, splenic tumors from IGF-IR dom-neg–transfected cells were significantly smaller (mean ± SEM: parental, 72.6 mm^3 ± 22.49 mm^3; pcDNA3, 97.4 mm^3 ± 49.38 mm^3; IGF-IR dom-neg, 2.2 mm^3 ± 0.56 mm^3; $p < 0.05$) and had a decreased mass (mean ± SEM: parental, 0.22 g ± 0.03 g; pcDNA3, 0.25 g ± 0.096 g; IGF-IR dom-neg, 0.12 g ± 0.005 g; $p < 0.05$).

A

B
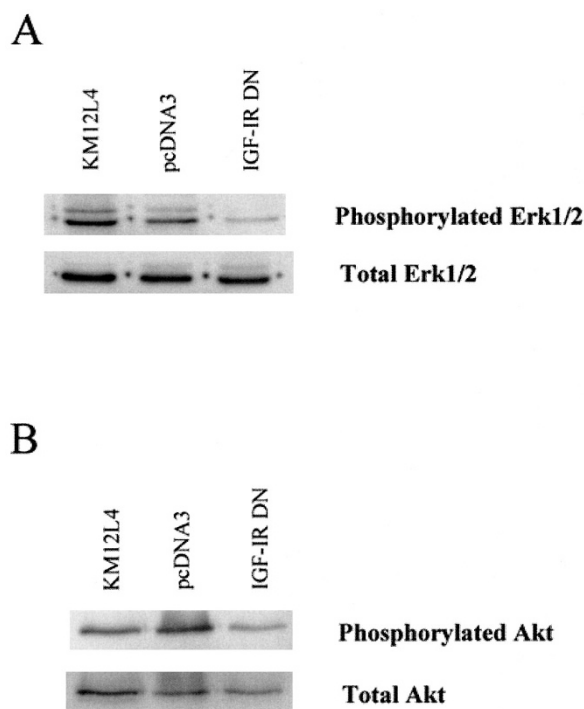
Figure 2.
Signaling pathways induced by IGF-I in IGF-IR dom-neg–transfected cells. Protein was extracted from growing KM12L4 parental and transfected cells, and Western blot analysis was performed. IGF-IR dom-neg–transfected cells showed decreased constitutive levels of phosphorylated Erk1/2 (A) and Akt (B) compared with parental and pcDNA3-transfected cells.

To verify the impact of IGF-IR dom-neg transfection on tumor growth in the liver, cells were injected directly into the liver (10–11 mice/group). After 16 days, mice in the control groups became moribund, and all mice were killed. Although most parental cells (6/10) and mock transfectants (8/11) formed liver tumors, there were no visible tumors in mice injected with IGF-IR dom-neg–transfected cells (0/10; $p < 0.05$; χ^2 analysis) (Fig. 4). In addition, livers from the control groups had a greater mass compared with those of the IGF-IR dom-neg group (mean $\pm$ SEM: parental, 1.7 g $\pm$ 0.077 g; pcDNA3, 1.95 g $\pm$ 0.256 g; IGF-IR dom-neg, 1.44 g $\pm$ 0.055 g; $p < 0.05$).

Impact of IGF-IR dom-neg Transfection on Proliferation, VEGF Expression, Vessel Counts, and Pericyte Coverage In Vivo

To further determine the effect of IGF-IR dom-neg transfection in vivo, subcutaneously grown tumors were analyzed by immunohistochemical analysis (Fig. 5). Examination of hematoxylin and eosin (HE)–stained sections demonstrated that the tissue morphology of tumors from IGF-IR dom-neg–transfected cells was distinct from that of control tumors, with the former demonstrating prominent connective tissue. Further immunohistochemical analyses demonstrated that tumors from IGF-IR dom-neg–transfected cells had significantly decreased cell proliferation (proliferating cell nuclear antigen; PCNA) ($\sim \uparrow$ 43–45%; $p < 0.0001$) and enhanced tumor cell apoptosis (TdT-mediated dUTP nicked-end labeling; TUNEL) ($\sim \downarrow$ 43–67%; $p < 0.05$) compared with controls (parental cells and mock transfectants, respectively). Immunofluorescent staining demonstrated that the phosphorylation of Erk1/2 and Akt was decreased in tumors derived from IGF-IR dom-neg–transfected cells compared with controls (not shown). In all the above analyses, there were no significant differences between the two controls groups (tumors from KM12L4 parental and pcDNA3-transfected cells).

To study the effect of IGF-IR dom-neg transfection on tumor angiogenesis in vivo, we stained the subcutaneously grown tumors for VEGF expression using an antibody that recognizes the VEGF 165, 189, and 206 isoforms. By image analysis, tumor cells with impaired IGF-IR function demonstrated significantly less VEGF staining intensity ($\sim$19–23%) than did controls ($p < 0.01$), consistent with our findings in vitro. In additional studies, vessels were highlighted with antibodies to CD31 and counted. In general, the morphology of vessels in tumors from IGF-IR dom-neg–transfected cells seemed to be vastly different from that of control tumors, with the former having a smaller diameter and more irregular shape (Fig. 6). Furthermore, the number of vessels was significantly decreased ($p < 0.05$; Fig. 7A). Because the morphology of the vessels suggested a change in endothelial cell structure, we performed concurrent staining for vessels and pericytes (working on the assumption that peri-CD31, α-smooth muscle actin [SMA]-positive cells were pericytes). Pericytes are hypothesized to exert an important stabilizing function on endothelial cells (Hirschi and D'Amore, 1997; Hirschi et al, 1999; Reinmuth et al, 2001). In tumors from IGF-IR dom-neg–transfected cells, the percentage of CD31-positive endothelial cells covered by pericytes was significantly decreased compared with both control groups ($p < 0.05$; Fig. 7B). Representative pictures are displayed in Figure 5.

Effect of Conditioned Medium on hVSMC Migration

Because we found a decrease in pericyte coverage in the tumors from IGF-IR dom-neg–transfected cells in vivo, we investigated the effect of KM12L4-derived conditioned medium on the migration of hVSMC in vitro. hVSMCs were seeded in modified Boyden chambers in conditioned medium, and migration was determined after 24 hours. hVSMCs exposed to conditioned medium derived from IGF-IR dom-neg–transfected cells migrated significantly less than cells in conditioned medium from parental and mock-transfected cells ($\sim \downarrow$ 53–57%; $p < 0.001$). This effect was not likely caused by alterations in platelet-derived growth factor-BB (PDGF-BB) or transforming growth factor-β (TGF-β) protein levels (known modulators of smooth muscle cell functions; Hirschi et al, 1999; Pukac et al, 1998; Salm et al, 2000) because Western blot analysis of concentrated conditioned medium showed no differences in the levels of these proteins between IGF-IR dom-neg–transfected cells and controls (not shown).

A

B
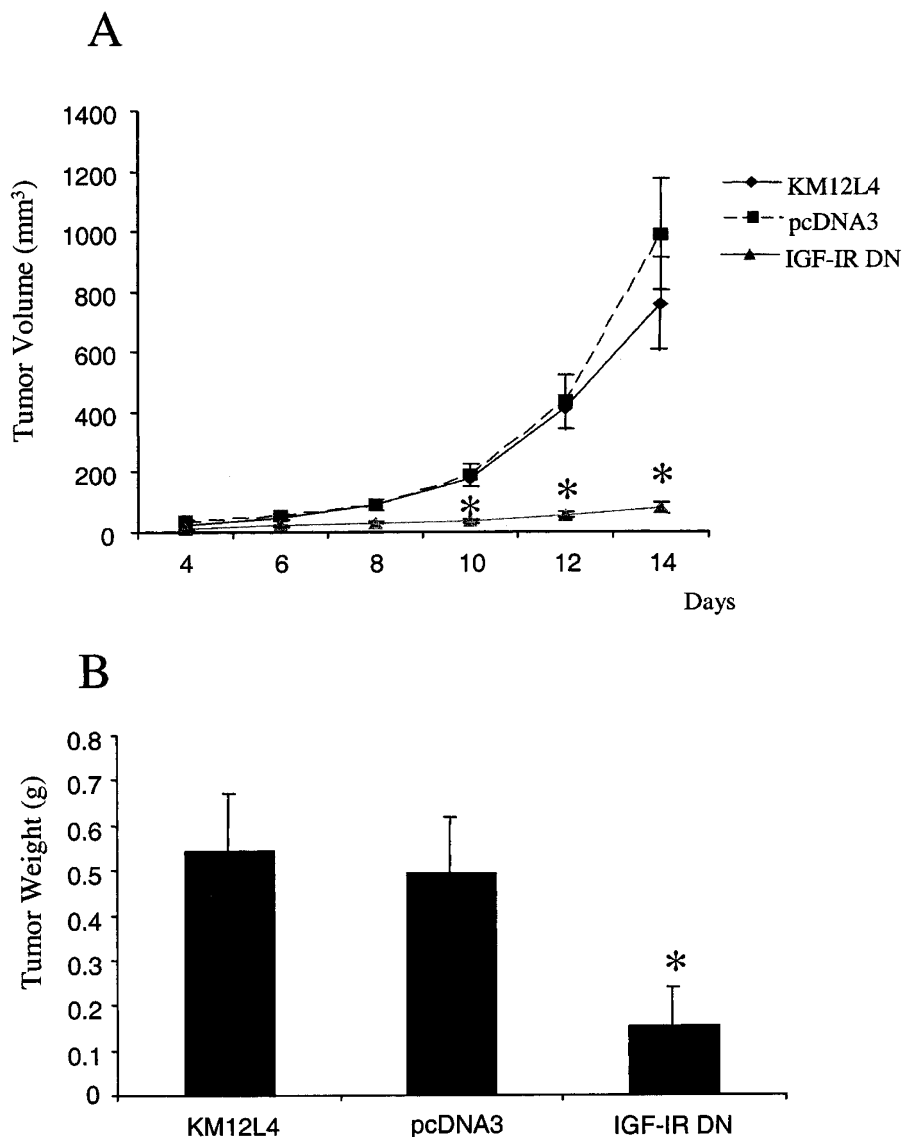
Figure 3.
Tumor growth of IGF-IR dom-neg–transfected cells in nude mice. Parental and transfected KM12L4 cells were injected subcutaneously into nude mice (10/group). After 14 days, tumors were harvested. A, Cells with decreased IGF-IR function (*IGF-IR DN*) demonstrated inhibited growth compared with parental and pcDNA3-transfected cells (*$p < 0.001$). B, Tumors derived from IGF-IR dom-neg–transfected cells weighed significantly less than tumors in the control groups (*bars*: mean ± SEM; *$p < 0.05$).

Discussion

The IGF-IR is a member of the large family of protein-tyrosine kinases that play a pivotal role in normal and abnormal processes including DNA synthesis, cell proliferation, differentiation, and survival (Baserga et al, 1997a, 1997c; Rubin and Baserga, 1995; Werner and Le Roith, 1997). However, the vast majority of studies on IGF-IR have been done in vitro; the importance of IGF-IR in vivo, particularly for human colon cancer, remains largely unknown. In a recent study on human colon cancer specimens, the increased expression of IGF-IR was correlated with higher tumor grade and higher-stage tumors (Hakam et al, 1999). Our laboratory previously demonstrated that IGF-I increases VEGF expression in human colon carcinoma cells, suggesting the possible involvement of IGF-IR in

angiogenesis (Akagi et al, 1998). This observation is of particular interest because the organ with the highest constitutive levels of IGF-I, the liver (Singh and Rubin, 1993), is also the most common site of distant metastasis from colon cancer. In addition to having a paracrine effect, IGF-I and IGF-II may also act in an autocrine manner because colon mucosa and colon cancers themselves synthesize significant amounts of IGF-I (Hakam et al, 1999).

To evaluate the importance of IGF-IR in human colon cancer and particularly its contribution to tumor angiogenesis, we stably transfected KM12L4 colon cancer cells with a truncated IGF-IR. This truncated receptor lacks the cytosolic tyrosine kinase domain and forms heterodimers with wild-type IGF-IR, thereby impairing its function (Prager et al, 1992, 1994). Pa-

Subcutaneous Tumor

Direct Liver Injection

## Liver Metastasis Model
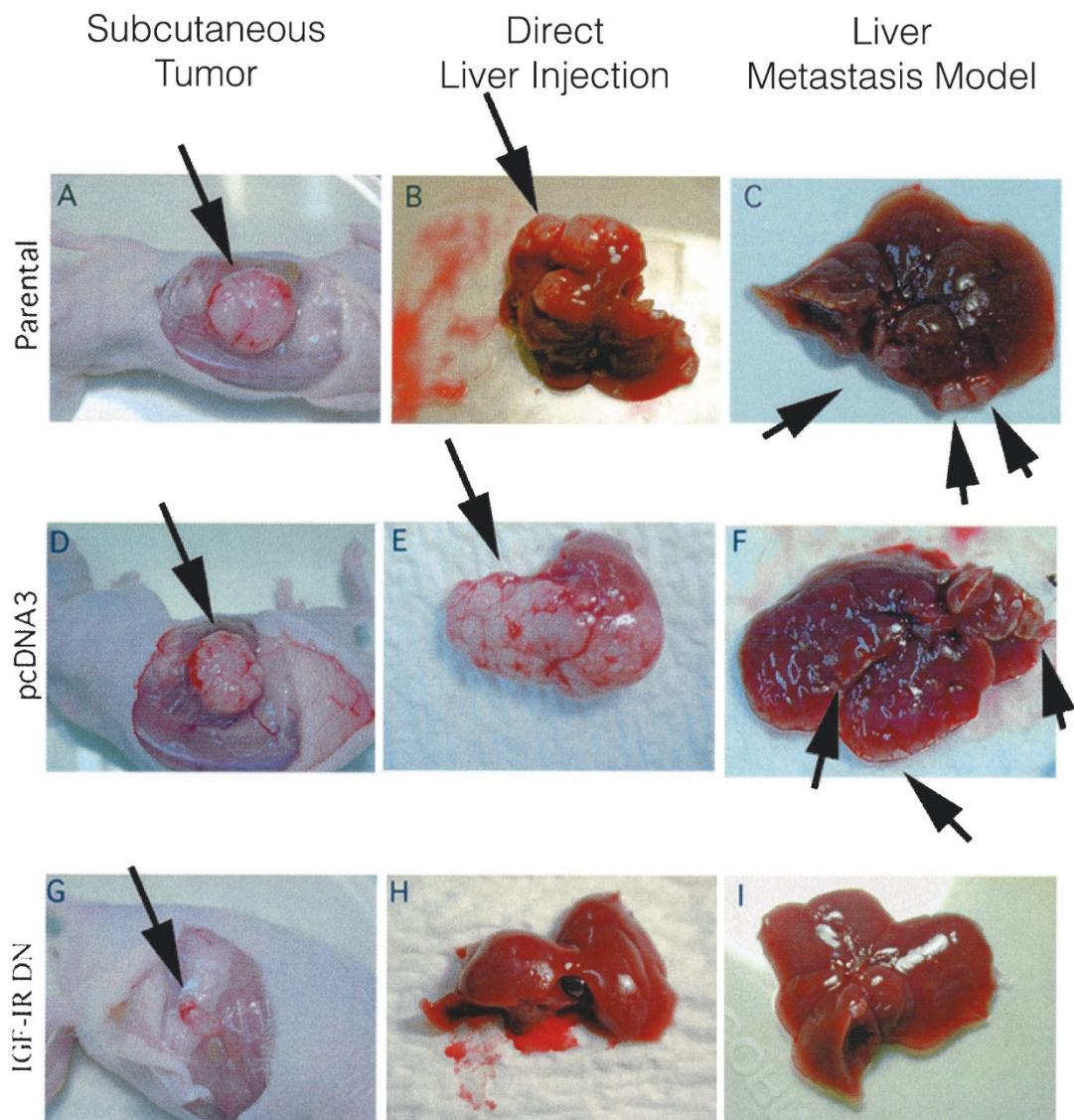
Figure 4.

Tumor growth and metastasis formation of parental and transfected KM12L4 cells in vivo. The growth and metastasis of parental and transfected (*pcDNA3* and *IGF-IR DN*) cells were studied in several experiments. Cells were injected subcutaneously (A, D, and G), directly into the liver (B, E, and H), or into the spleen (to form liver metastases) (C, F, and I). The experiment was terminated when control mice became moribund. Representative pictures demonstrate that IGF-IR dom-neg–transfected cells had decreased tumor growth in the subcutis (G) and no tumor development in the liver (H). In addition, liver metastases were completely absent in mice injected with IGF-IR dom-neg–transfected cells (I). *Arrows* point to representative tumors.

rental KM12L4 cells constitutively expressed a high amount of VEGF mRNA that was similar to the levels expressed in mock transfectants. In contrast, transfection with the IGF-IR dom-neg construct led to a marked decrease in constitutive VEGF expression. As confirmed by RT-PCR, all VEGF isoforms were decreased in IGF-IR dom-neg–transfected cells. In addition, these cells also secreted markedly less VEGF protein compared with controls. Incubation of parental and mock-transfected cells with IGF-I further increased VEGF mRNA and protein expression, whereas in IGF-IR dom-neg–transfected cells, VEGF mRNA and protein could be stimulated by IGF-I only to a minor extent and remained strongly decreased. Furthermore, constitutive activation of both the MAPK (Erk) and PI-3K (Akt) pathways was decreased in

IGF-IR dom-neg–transfected cells, as indicated by Western blot analysis. Although several intracellular pathways have been reported to be activated by IGF-I through the IGF-IR (Baserga et al, 1997a; Kim et al, 1998; Miele et al, 2000; Werner and Le Roith, 1997), the MAPK pathway has been shown to be essential for VEGF induction (Miele et al, 2000). In addition, the MAPK and PI-3K pathways seem to be involved in regulating proliferation and survival, respectively (Miele et al, 2000; Satyamoorthy et al, 2001; Solorzano et al, 2001).

Transfection with a truncated IGF-IR had a significant effect on tumor growth and development. Monolayer cell growth in vitro was moderately inhibited by IGF-IR dom-neg transfection, a finding similar to other reports (Dunn et al, 1998; Reiss et al, 1998). More
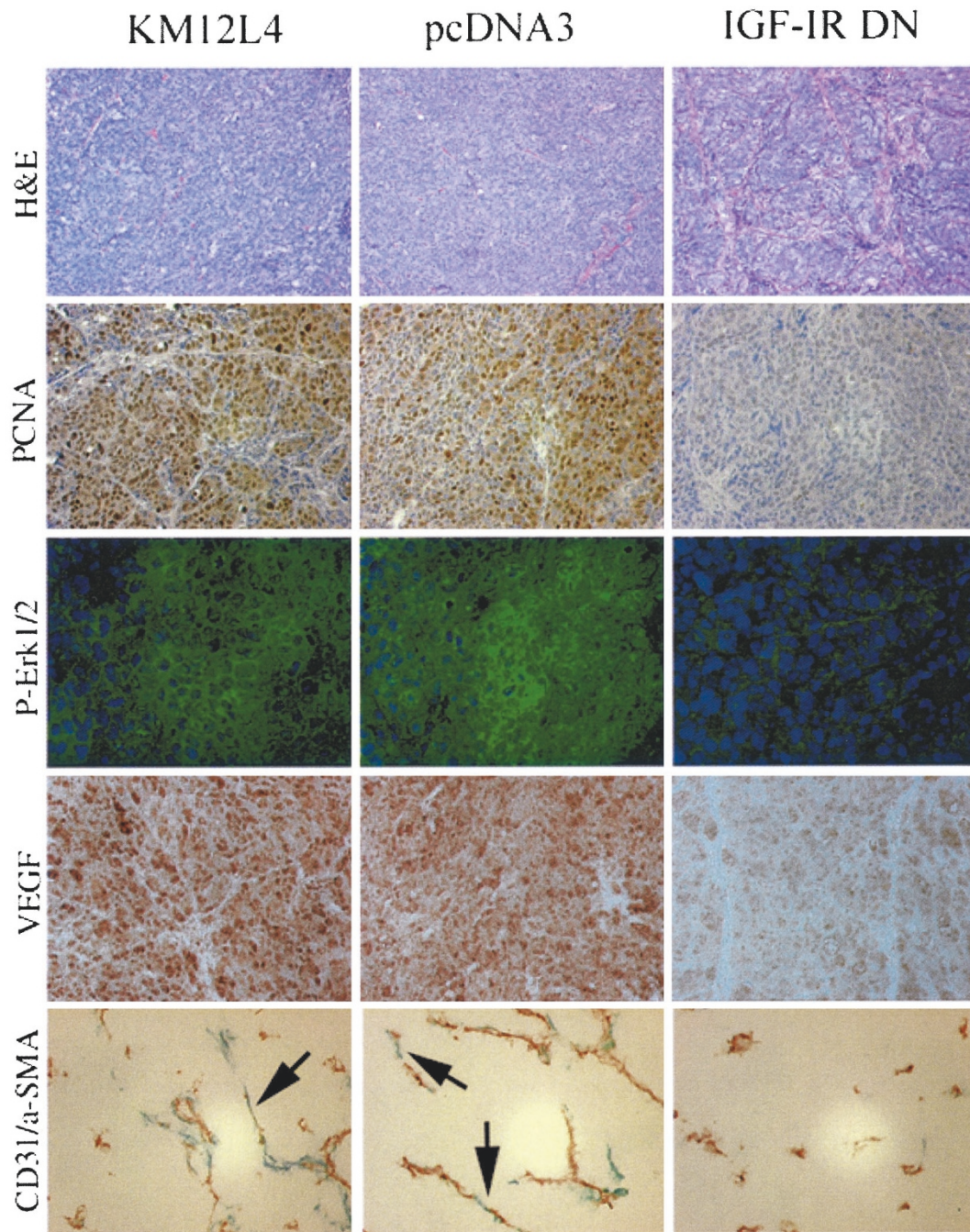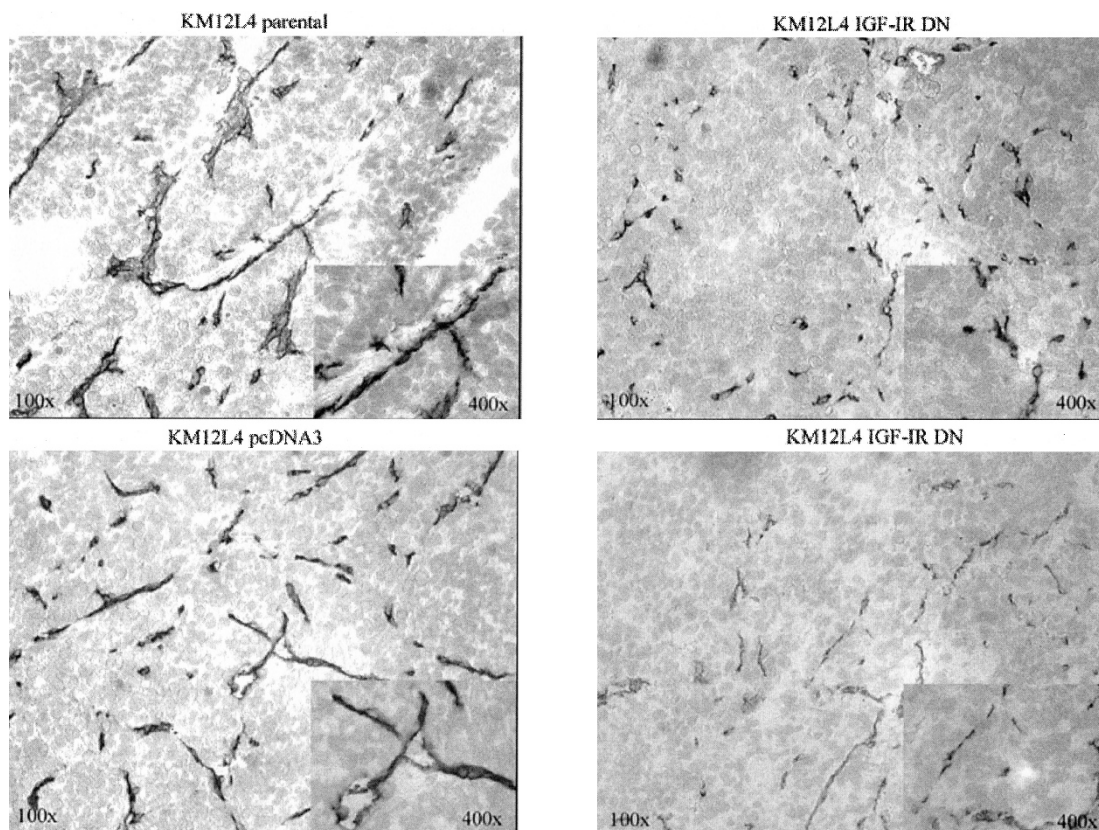
Figure 5.
Immunohistochemical analysis of parental and transfected KM12L4 cells grown in the subcutis. Parental and transfected (*pcDNA3* and *IGF-IR DN*) cells were grown subcutaneously in nude mice. Tumors were harvested and stained with hematoxylin and eosin (*H&E*) and antibodies to proliferating cell nuclear antigen (*PCNA*) (brown), phosphorylated Erk1/2 (green), VEGF (brown), CD31 (brown), and α-smooth muscle actin (*SMA*) (blue) (*arrows* point to pericyte coverage of vessels). Representative areas are shown (for HE and PCNA: magnification ×50; for phosphorylated Erk1/2, VEGF, and α-SMA/CD31 double-staining: magnification ×200).

important, the growth of IGF-IR dom-neg–transfected cells in vivo was markedly impaired. After injection into the subcutis, IGF-IR dom-neg–transfected cells formed tumors that were significantly smaller and had a significantly decreased mass compared with the control groups. These findings are consistent with previous studies in other tumor systems using a modified IGF-IR construct to alter IGF-IR function (Prager et al, 1994; Reiss et al, 1998). Furthermore, metastasis formation by human colon cancer cells

transfected with IGF-IR dom-neg and injected intrasplenically was completely abrogated. To confirm that this effect was a result of impaired tumor development in the liver, cells were injected directly into the liver. IGF-IR dom-neg–transfected cells similarly failed to form macroscopically visible liver tumors. In contrast, the tumorigenicity of mock-transfected cells was similar to that of parental cells. These findings are in agreement with those of a recent study on the role of IGF-IR in human breast cancer cells (Dunn et al, 1998).
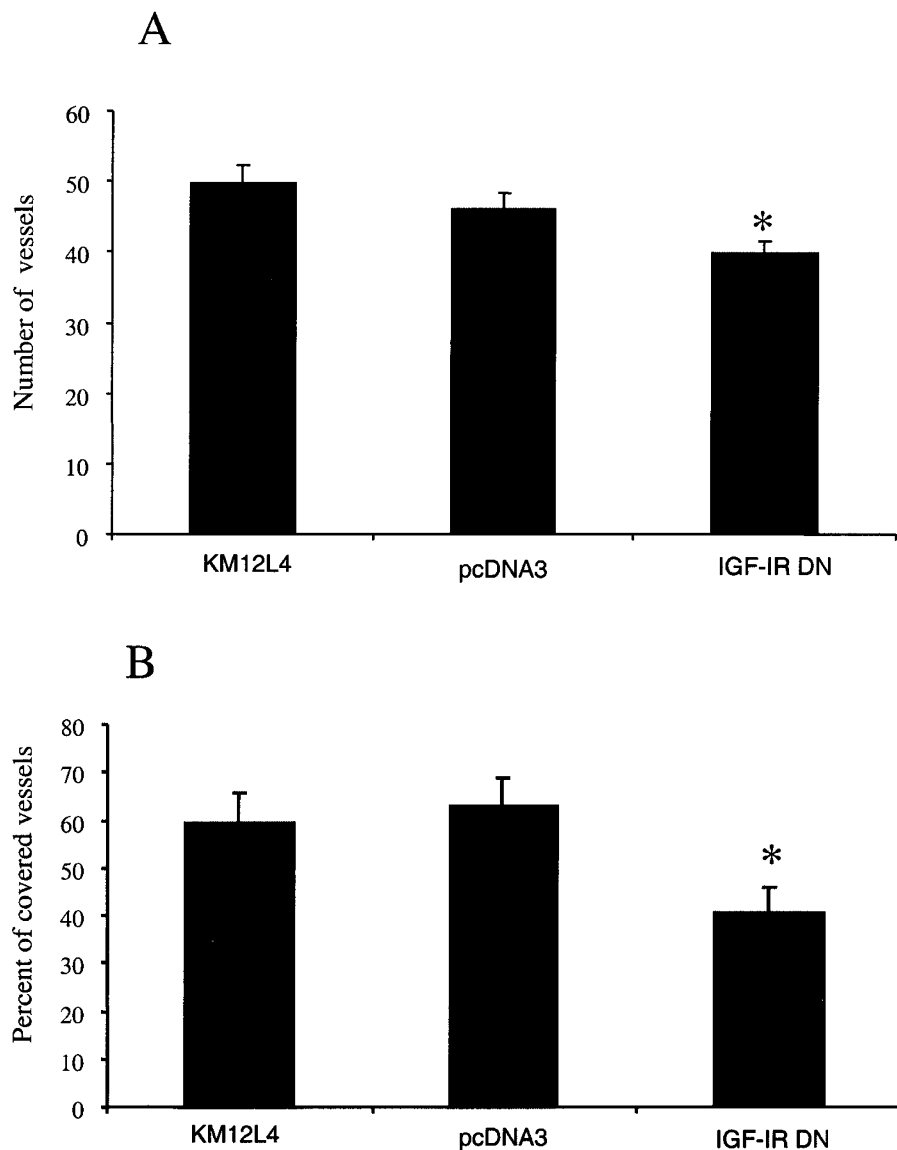
Figure 6.
Immunohistochemical analysis of microvessel density in subcutaneous tumors (stained with CD31) derived from parental and transfected KM12L4. Representative pictures are shown at ×100 and, to better demonstrate differences, at ×400 magnification. Tumors from IGF-IR dom-neg–transfected cells (*IGF-IR DN*) demonstrated a distinct vessel architecture, with most vessels being smaller in diameter and more irregular in shape than in tumors from parental and pcDNA3-transfected cells.

Immunohistochemical analyses of subcutaneously grown tumors demonstrated markedly decreased proliferation and increased apoptosis in IGF-IR dom-neg–transfected cells. Similarly, the activation status of the MAPK and PI-3K pathways was also decreased in these tumors, indicating impaired signaling involved in proliferation and apoptosis (Satyamoorthy et al, 2001; Solorzano et al, 2001).

Because previous work demonstrated that IGF-I led to an increase in VEGF expression (Akagi et al, 1998; Warren et al, 1996; Wu et al, 2002), we determined the effect of IGF-IR dom-neg transfection on tumor angiogenesis in vivo. Because the most active angiogenic site in tumors is the interface between the tumor and normal tissue (Takahashi et al, 1995), we assessed VEGF expression and microvessel counts in this region in subcutaneous tumors in nude mice. IGF-IR dom-neg–transfected cells expressed significantly less VEGF and showed significantly fewer vessels than did control tumors. These findings are consistent with those of Wu and associates who demonstrated that mice with higher circulating IGF-I levels had more intense VEGF expression in vivo (Wu et al, 2002). Because IGF-IR function in tumor cells modulated angiogenesis, we investigated in more detail the morphology of the tumor vasculature. In tumors from IGF-IR dom-neg–transfected cells, vessel morphology appeared to be vastly different, suggesting an alter-

ation in vessel structure. Pericytes are known to be closely associated to endothelial cells and are critical for proper vascular development and maintenance (Hirschi et al, 1999; Reinmuth et al, 2001). Colocalized endothelial cells and pericytes have recently been used to define "mature" blood vessels (Eberhard et al, 2000). Since pericytes are also present in tumor vessels to varying degrees (Eberhard et al, 2000), we developed an immunohistochemical method to study the colocalization of perivascular cells and endothelial cells. In tumors from IGF-IR dom-neg–transfected cells, pericyte coverage was significantly decreased. Therefore, targeting the IGF-IR on colon cancer cells may not only decrease VEGF expression (a major mitogen and survival factor for endothelial cells) but also affect pericytes in a paracrine manner. To further evaluate this hypothesis, we studied the effect of colon cancer–derived conditioned medium on the migration of hVSMCs as surrogates for pericytes. hVSMCs migrated significantly less when stimulated with conditioned medium derived from IGF-IR dom-neg–transfected cells than with conditioned medium from control cells. Recent reports indicate that hVSMCs express VEGF receptors (Ishida et al, 2001), and VEGF has also been reported to be a mitogen for hVSMCs (Grosskreutz et al, 1999). Therefore, the decreased VEGF concentration in conditioned medium derived from IGF-IR dom-neg–transfected cells

A

B

Figure 7.
Microvessel density and pericyte coverage in KM12L4-derived subcutaneous tumors. A, Tissue sections were stained with antibodies to CD31, and vessels in four distinct regions were counted at ×100 magnification. Vessels counts in tumors from IGF-IR dom-neg–transfected cells (*IGF-IR DN*) were significantly lower than in controls (*$p < 0.05$). B, Slides were double-stained with antibodies to α-SMA and CD31, and pericyte coverage was determined as described in "Materials and Methods." The percentage of pericyte-covered vessels was significantly lower in tumors from IGF-IR dom-neg–transfected cells than in tumors from parental and pcDNA3-transfected cells (*$p < 0.05$).

may have contributed to these results; however, cytokines other than VEGF also may have been involved. In contrast, PDGF-BB and TGF-β, which are known modulators of hVSMC migration and proliferation (Hirschi et al, 1999; Pukac et al, 1998; Salm et al, 2000), were not differentially secreted by IGF-IR dom-neg–transfected cells compared with control cells.

Our data demonstrate the critical role of IGF-IR in colon cancer growth and metastasis. Furthermore, this report is the first to demonstrate that inhibiting IGF-IR function in cancer cells may be an indirect means of inhibiting angiogenesis by decreasing VEGF expression and pericyte coverage. Inhibition of a threshold level of the IGF-IR might be sufficient to affect multiple IGF-IR functions (Butler et al, 1998). Therefore, this receptor seems to be a promising

target for human colon cancer therapy. Additional studies are clearly needed to further understand the complex IGF system, including the IGF-IR, and to evaluate the IGF-IR as a target in cancer therapy.

Materials and Methods

Materials

Recombinant human IGF-I was purchased from R&D Systems, Inc. (Minneapolis, Minnesota). The following antibodies were used for immunohistochemical and Western blot analyses: monoclonal mouse anti-PCNA clone PC10 (Dako A/S, Glostrup, Denmark); monoclonal rat anti-mouse CD31 (PharMingen, San Diego, California); polyclonal rabbit anti-phospho-p44/42

MAPK (Cell Signaling Technology, Beverly, Massachusetts); polyclonal rabbit MAPK (Oncogene Research Products, Cambridge, Massachusetts); monoclonal mouse anti-human VEGF recognizing the 165, 189, and 206 amino acid isoforms (PharMingen); goat anti-mouse IgG (Jackson Research Laboratories, West Grove, Pennsylvania); horseradish peroxidase–conjugated (HRP) goat anti-rat IgG and Texas Red–conjugated goat anti-rat IgG (Jackson Research Laboratories); HRP rat anti-mouse IgG2a (Serotec, Harlan Bioproducts for Science, Inc., Indianapolis, Indiana); HRP goat anti-mouse IgG (Jackson Research Laboratories), HRP anti-mouse IgG (PharMingen); polyclonal rabbit anti-IGF-IRα (Santa Cruz Biotechnology, Santa Cruz, California); polyclonal rabbit anti-IGF-IRβ (Santa Cruz Biotechnology); HRP goat anti-rabbit IgG (Bio-Rad Laboratories, Hercules, California); rabbit anti-human phosphorylated Akt and Akt (Ser473; Cell Signaling Technology); rabbit anti-human TGF-β (R&D Systems); rabbit anti-human PDGF-B (Santa Cruz Biotechnology); and mouse anti-human anti-α-SMA (Dako, Carpinteria, California).

Cell Lines and Culture Conditions

Human KM12L4 colon cancer cells were obtained from I. J. Fidler, D.V.M., Ph.D. (The University of Texas M. D. Anderson Cancer Center) (Morikawa et al, 1988); cells were maintained as previously described (Shaheen et al, 2001). hVSMCs were purchased from the American Type Culture Collection (Manassas, Virginia) and were maintained as previously described (Reinmuth et al, 2001). All in vitro experiments were performed at least in triplicate at 50% to 60% cell confluence. A mutated IGF-IR truncated at position 952 in the β subunit transmembrane region (IGF-IR dom-neg) was the generous gift of D. Prager, MD (Cedars-Sinai Medical Center, UCLA School of Medicine, Los Angeles, California) (Prager et al, 1992, 1994). IGF-IR dom-neg was subcloned into the pcDNA3 vector (Invitrogen Corporation, Carlsbad, California) containing a neomycin (G418; Life Technologies, Grand Island, New York) resistance gene. The resulting vector was stably transfected into human KM12L4 colon cancer cells using FuGENE 6 transfection reagent (Roche Diagnostics Corporation, Indianapolis, Indiana) following the manufacturer's protocol. Transfected clones were expanded and cultured in 600 μg/mL G418-containing medium. To confirm successful transfection, cell extracts of parental and transfected cells were analyzed by nondenaturing Western blot analysis using anti-IGF-IRα and anti-IGF-IRβ antibodies.

VEGF Induction in Transfected Cells

Parental and transfected cells were grown to 50% to 60% confluence in standard medium (Shaheen et al, 2001) as described above. The medium was then changed to 5% fetal bovine serum (FBS)–containing medium, and the cells were incubated overnight. Cells were then incubated in the presence or absence of IGF-I (100 ng/mL) in serum-free medium for 24 hours. Total RNA was extracted, and VEGF mRNA expression was determined by Northern blot analysis and semiquantitative RT-PCR as described previously (Ellis et al, 1996; Koura et al, 1996). The cDNA probes used were as follows: a human VEGF-specific 204-bp cDNA probe (a generous gift of B. Berse, PhD, Harvard Medical School, Boston, Massachusetts) (Berse et al, 1992) and a glyceraldehyde-3-phosphate dehydrogenase probe (purchased from American Type Culture Collection). The VEGF probe identifies all alternatively spliced forms of its mRNA transcripts. In a separate experiment designed to evaluate VEGF protein expression, conditioned medium was harvested after 48 hours from cells growing in 1% FBS-containing medium with or without IGF-I (100 ng/mL). The VEGF concentration was determined using an ELISA kit for human VEGF (R&D Systems) as previously reported (Reinmuth et al, 2001) (the ELISA kit recognizes the VEGF121 and VEGF165 isoforms of the protein; Cheng et al, 1997).

Effect of IGF-IR dom-neg Transfection on Signaling Pathways

Parental and transfected cells were grown to 50% confluence, the medium was changed to 5% FBS-containing medium, and the cells were incubated overnight. Cells were then harvested, and protein was extracted. To determine the effect of IGF-IR dom-neg transfection on signaling pathways, Western blot analysis was performed using antibodies against phosphorylated and total forms of p44/42 (Erk1/2) and Akt as previously described (Reinmuth et al, 2001).

Effect of IGF-IR dom-neg Transfection on Monolayer Cell Growth

To determine the effect of IGF-IR dom-neg transfection on monolayer cell growth, 10^4 KM12L4 cells were plated in 96-well plates. After cell attachment, the medium was changed to 10% FBS-containing medium for 48 hours. MTT (Sigma, St. Louis, Missouri) was added to a final concentration of 0.5 mg/mL, and cells were incubated for 90 minutes. The medium and MTT were removed, dimethyl sulfoxide was added for 1 minute, and absorption was read at 570 nm.

In Vivo Studies

Eight-week-old male nude mice were purchased from the Animal Production Area of the National Cancer Institute-Frederick Cancer Research and Development Center (Frederick, Maryland) and housed as previously described (Bruns et al, 2000b). Mice were acclimated for 1 to 2 weeks. For in vivo injections, KM12L4 parental and pcDNA3 and IGF-IR dom-neg transfected human colon cancer cells (total three groups; $n = 9$–11/group) were grown to 50% confluence, incubated in G418-free medium for 24 hours to negate the effect of G418 on the growth of implanted tumor cells, and harvested as described (Ellis et al, 1996). To study the effect of IGF-IR dom-neg trans-

fection on tumor growth, single-cell suspensions (200 μl containing 10^6 cells) of >90% viability (Shaheen et al, 1999, 2001) were injected subcutaneously through a 27-gauge needle into the right flank. In another experiment designed to determine the role of IGF-IR on tumor growth in the liver, cell suspensions (50 μl containing 10^6 cells) were injected beneath the capsule into the left lobe of the liver or into the spleen of nude mice via a midline incision using a 30-gauge needle (Morikawa et al, 1988). All mice in all groups were killed when three or more mice in any group became moribund or when subcutaneous tumors exceeded 1.2 cm in diameter. Necropsy procedures were performed as described (Bruns et al, 2000b).

For evaluation of tumor growth in the liver, the liver was excised and weighed, and the number of liver metastases was counted. The two-dimensional diameters of the largest tumor in each liver were measured, and the tumor volume was estimated using the equation: volume = 0.5*(long diameter)*(short diameter)^2. If no tumor was visible, the liver was serially sectioned at 1-mm intervals to search for minute tumors within the parenchyma.

Immunohistochemical Analyses

Immunohistochemical staining for HE staining (to study overall tissue structure) and determination of expression of PCNA and VEGF was performed on paraffin-embedded tissues as previously described (Bruns et al, 2000b; Takahashi et al, 1998) using stable diaminobenzidine (Research Genetics, Huntsville, Alabama) as the substrate. Sections were counterstained with Gill's 3 hematoxylin (Sigma) and mounted with Universal Mount (Research Genetics). For analysis of VEGF expression, the signal was amplified using the TSA Biotin System (NEN Life Science, Boston, Massachusetts), and counterstaining was omitted.

Immunohistochemical analysis for CD31 (endothelial cells) was done on frozen tissue sections as previously described (Shaheen et al, 1999). For determination of pericyte coverage, double-staining for CD31 and α-SMA was performed similar to the procedure described by Eberhard et al (2000). For all staining procedures, negative controls were prepared by omission of the primary antibody.

For immunofluorescent staining, frozen sections of tumor (8-μm thick) were fixed in cold acetone and chloroform, washed with phosphate-buffered saline, and incubated with primary and secondary antibodies as previously described (Bruns et al, 2000b; Shaheen et al, 1999; Solorzano et al, 2001). The TUNEL assay was performed with a commercial kit (Promega, Madison, Wisconsin) according to the manufacturer's protocol. CD31 and TUNEL double-staining was performed where endothelial cells were identified by red fluorescence (CD31-positive). DNA fragmentation (TUNEL positive) was detected in tumor and endothelial cells by localized green (TUNEL-positive) and yellow (TUNEL- and CD31-positive) fluorescence, respectively.

Quantification of PCNA, TUNEL, and VEGF Staining

For evaluation of immunohistochemical staining in tumors grown in mice, only the tumor edge was examined to avoid geographic bias. Morphologically necrotic areas were excluded. The numbers of PCNA- and TUNEL-positive tumor cells were counted in four areas containing the highest expression at ×200 and ×100 magnification, respectively. The intensity of VEGF staining was graded by computer-assisted image analysis with Optimas software (Media Cybernetics, Silver Spring, Maryland). The image was converted into a grayscale image for measurement of the optical density, and four distinct areas with high VEGF expression were evaluated at ×100 magnification. To validate the image analysis system, all sections were also semiquantitatively scored subjectively as previously described (Takahashi et al, 1995, 1998). No differences between the objective and subjective techniques were found.

Quantification of Microvessel Density and Pericyte Coverage

The number of microvessels at the tumor edge was counted in four quadrants at ×100 magnification according to the method described by Weidner (1995). Necrotic areas were excluded. The percentage of pericyte-covered vessels was then determined by the method of Eberhard and coworkers at four distinct high-density areas ("hot spots") near the tumor edge at ×200 magnification [% pericyte coverage = (number of tumor microvessels that demonstrate pericyte colocalization/total number of tumor microvessels) × 100] (Eberhard et al, 2000). (Pericytes were defined as a single layer of α-SMA–positive cells surrounding CD31-positive cells.) Large tumor vessels were excluded from this analysis because any colocalized staining for α-SMA in this setting could be a result of expression by VSMCs and not necessarily pericytes (Eberhard et al, 2000).

hVSMC Migration Assay

Conditioned medium was collected from parental and transfected KM12L4 cells, centrifuged at 2000 rpm for 5 minutes at room temperature, and filtered through a 0.22-μm filter. The migration assay was performed using modified Boyden chambers. Forty thousand hVSMCs in conditioned medium were seeded in 8.0-μm PET Membrane Inserts (Becton Dickinson Labware, Franklin Lakes, New Jersey) that were placed into 24-well plates (Becton Dickinson) containing conditioned medium. After 24 hours, nonmigrated cells on the top side of the inserts were removed with a cotton swab, and migrated cells on the underside of the insert were stained using a HEMA-3 kit (Biochemical Sciences, Swedesboro, New Jersey) and counted in five distinct regions at ×100 magnification. To determine a possible difference for the content of PDGF-BB or TGF-β in the conditioned medium derived from parental and transfected KM12L4 cells,

Western blot analyses were performed for these factors (Reinmuth et al, 2001).

Densitometric Quantification and Statistical Analysis

Densitometric analysis was performed using software from the National Institutes of Health (Bethesda, Maryland) to quantify the results of Northern blot analyses in the linear range of the film. Glyceraldehyde-3-phosphate dehydrogenase mRNA was used as an internal control for loading. All statistical analyses were performed using InStat statistical software (GraphPad Software, San Diego, California), with $p \leq$ 0.05 considered to be significant. For comparing tumor-associated parameters, the nonpaired Student's t test was used if not otherwise specified. If the standard deviations of two Gaussian distributions were significantly different, the alternate Welch t test was used. The χ^2 test was applied for comparing frequencies of developing liver tumors in nude mice.

Acknowledgements

References

Akagi Y, Liu W, Zebrowski B, Xie K, and Ellis LM (1998). Regulation of vascular endothelial growth factor expression in human colon cancer by insulin-like growth factor-I. Cancer Res 58:4008–4014.

Baserga R, Hongo A, Rubini M, Prisco M, and Valentinis B (1997a). The IGF-I receptor in cell growth, transformation and apoptosis. Biochim Biophys Acta 1332:F105–F126.

Baserga R, Resnicoff M, D'Ambrosio C, and Valentinis B (1997b). The role of the IGF-I receptor in apoptosis. Vitam Horm 53:65–98.

Baserga R, Resnicoff M, and Dews M (1997c). The IGF-I receptor and cancer. Endocrine 7:99–102.

Berse B, Brown LF, Van de Water L, Dvorak HF, and Senger DR (1992). Vascular permeability factor (vascular endothelial growth factor) gene is expressed differentially in normal tissues, macrophages, and tumors. Mol Biol Cell 3:211–220.

Brown LF, Detmar M, Claffey K, Nagy JA, Feng D, Dvorak AM, and Dvorak HF (1997). Vascular permeability factor/vascular endothelial growth factor: A multifunctional angiogenic cytokine. EXS 79:233–269.

Bruns CJ, Liu W, Davis DW, Shaheen RM, McConkey DJ, Wilson MR, Bucana CD, Hicklin DJ, and Ellis LM (2000a). Vascular endothelial growth factor is an in vivo survival factor for tumor endothelium in a murine model of colorectal carcinoma liver metastases. Cancer 89:488–499.

Bruns CJ, Solorzano CC, Harbison MT, Ozawa S, Tsan R, Fan D, Abbruzzese J, Traxler P, Buchdunger E, Radinsky R, and Fidler IJ (2000b). Blockade of the epidermal growth factor receptor signaling by a novel tyrosine kinase inhibitor leads to apoptosis of endothelial cells and therapy of human pancreatic carcinoma. Cancer Res 60:2926–2935.

Butler AA, Blakesley VA, Poulaki V, Tsokos M, Wood TL, LeRoith D, and Pouliki V (1998). Stimulation of tumor growth by recombinant human insulin-like growth factor-I (IGF-I) is dependent on the dose and the level of IGF-I receptor expression [published erratum appears in Cancer Res 1998 Dec 1;58(23):5630]. Cancer Res 58:3021–3027.

Cheng SY, Nagane M, Huang HS, and Cavenee WK (1997). Intracerebral tumor-associated hemorrhage caused by overexpression of the vascular endothelial growth factor isoforms VEGF121 and VEGF165 but not VEGF189. Proc Natl Acad Sci USA 94:12081–12087.

Dunn SE, Ehrlich M, Sharp NJ, Reiss K, Solomon G, Hawkins R, Baserga R, and Barrett JC (1998). A dominant negative mutant of the insulin-like growth factor-I receptor inhibits the adhesion, invasion, and metastasis of breast cancer. Cancer Res 58:3353–3361.

Eberhard A, Kahlert S, Goede V, Hemmerlein B, Plate KH, and Augustin HG (2000). Heterogeneity of angiogenesis and blood vessel maturation in human tumors: Implications for antiangiogenic tumor therapies. Cancer Res 60:1388–1393.

Ellis LM and Fidler IJ (1996). Angiogenesis and metastasis. Eur J Cancer 32A:2451–2460.

Ellis LM, Liu W, and Wilson M (1996). Down-regulation of vascular endothelial growth factor in human colon carcinoma cell lines by antisense transfection decreases endothelial cell proliferation. Surgery 120:871–878.

Ellis LM, Takahashi Y, Liu W, and Shaheen RM (2000). Vascular endothelial growth factor in human colon cancer: Biology and therapeutic implications. Oncologist 5:11–15.

Folkman J (1992). The role of angiogenesis in tumor growth. Semin Cancer Biol 3:65–71.

Freier S, Weiss O, Eran M, Flyvbjerg A, Dahan R, Nephesh I, Safra T, Shiloni E, and Raz I (1999). Expression of the insulin-like growth factors and their receptors in adenocarcinoma of the colon. Gut 44:704–708.

Grosskreutz CL, Anand-Apte B, Duplaa C, Quinn TP, Terman BI, Zetter B, and D'Amore PA (1999). Vascular endothelial growth factor-induced migration of vascular smooth muscle cells in vitro. Microvasc Res 58:128–136.

Hakam A, Yeatman TJ, Lu L, Mora L, Marcet G, Nicosia SV, Karl RC, and Coppola D (1999). Expression of insulin-like growth factor-1 receptor in human colorectal cancer. Hum Pathol 30:1128–1133.

Hirschi KK and D'Amore PA (1997). Control of angiogenesis by the pericyte: Molecular mechanisms and significance. EXS 79:419–428.

Hirschi KK, Rohovsky SA, Beck LH, Smith SR, and D'Amore PA (1999). Endothelial cells modulate the proliferation of mural cell precursors via platelet-derived growth factor-BB and heterotypic cell contact. Circ Res 84:298–305.

Ishida A, Murray J, Saito Y, Kanthou C, Benzakour O, Shibuya M, and Wijelath ES (2001). Expression of vascular endothelial growth factor receptors in smooth muscle cells. J Cell Physiol 188:359–368.

Kim B, Cheng HL, Margolis B, and Feldman EL (1998). Insulin receptor substrate 2 and Shc play different roles in insulin-like growth factor I signaling. J Biol Chem 273:34543–34550.

Koura AN, Liu W, Kitadai Y, Singh RK, Radinsky R, and Ellis LM (1996). Regulation of vascular endothelial growth factor

expression in human colon carcinoma cells by cell density. Cancer Res 56:3891–3894.

Liu JP, Baker J, Perkins AS, Robertson EJ, and Efstratiadis A (1993). Mice carrying null mutations of the genes encoding insulin-like growth factor I (Igf-1) and type 1 IGF receptor (Igf1r). Cell 75:59–72.

Michell NP, Langman MJ, and Eggo MC (1997). Insulin-like growth factors and their binding proteins in human colonocytes: Preferential degradation of insulin-like growth factor binding protein 2 in colonic cancers. Br J Cancer 76:60–66.

Miele C, Rochford JJ, Filippa N, Giorgetti-Peraldi S, and Van Obberghen E (2000). Insulin and insulin-like growth factor-I induce vascular endothelial growth factor mRNA expression via different signaling pathways. J Biol Chem 275:21695–21702.

Morikawa K, Walker SM, Nakajima M, Pathak S, Jessup JM, and Fidler IJ (1988). Influence of organ environment on the growth, selection, and metastasis of human colon carcinoma cells in nude mice. Cancer Res 48:6863–6871.

Prager D, Li HL, Asa S, and Melmed S (1994). Dominant negative inhibition of tumorigenesis in vivo by human insulin-like growth factor I receptor mutant. Proc Natl Acad Sci USA 91:2181–2185.

Prager D, Yamasaki H, Weber MM, Gebremedhin S, and Melmed S (1992). Human insulin-like growth factor I receptor function in pituitary cells is suppressed by a dominant negative mutant. J Clin Invest 90:2117–2122.

Pukac L, Huangpu J, and Karnovsky MJ (1998). Platelet-derived growth factor-BB, insulin-like growth factor-I, and phorbol ester activate different signaling pathways for stimulation of vascular smooth muscle cell migration. Exp Cell Res 242:548–560.

Reinmuth N, Liu W, Jung YD, Ahmad SA, Shaheen RM, Fan F, Bucana CD, McMahon G, Gallick GE, and Ellis LM (2001). Induction of VEGF in perivascular cells defines a potential paracrine mechanism for endothelial cell survival. FASEB J 15:1239–1241.

Reiss K, D'Ambrosio C, Tu X, Tu C, and Baserga R (1998). Inhibition of tumor growth by a dominant negative mutant of the insulin-like growth factor I receptor with a bystander effect. Clin Cancer Res 4:2647–2655.

Rubin R and Baserga R (1995). Insulin-like growth factor-I receptor: Its role in cell proliferation, apoptosis, and tumorigenicity. Lab Invest 73:311–331.

Salm SN, Koikawa Y, Ogilvie V, Tsujimura A, Coetzee S, Moscatelli D, Moore E, Lepor H, Shapiro E, Sun TT, and Wilson EL (2000). Transforming growth factor-beta is an autocrine mitogen for a novel androgen-responsive murine prostatic smooth muscle cell line, PSMC1. J Cell Physiol 185:416–424.

Satyamoorthy K, Li G, Vaidya B, Patel D, and Herlyn M (2001). Insulin-like growth factor-1 induces survival and growth of biologically early melanoma cells through both the mitogen-activated protein kinase and beta-catenin pathways. Cancer Res 61:7318–7324.

Shaheen RM, Ahmad SA, Liu W, Reinmuth N, Jung YD, Tseng WW, Drazan KE, Bucana CD, Hicklin DJ, and Ellis LM (2001). Inhibited growth of colon cancer carcinomatosis by antibodies to vascular endothelial and epidermal growth factor receptors. Br J Cancer 85:584–589.

Shaheen RM, Davis DW, Liu W, Zebrowski BK, Wilson MR, Bucana CD, McConkey DJ, McMahon G, and Ellis LM (1999). Antiangiogenic therapy targeting the tyrosine kinase receptor for vascular endothelial growth factor receptor inhibits the growth of colon cancer liver metastasis and induces tumor and endothelial cell apoptosis. Cancer Res 59:5412–5416.

Singh P, Dai B, Dhruva B, and Widen SG (1994). Episomal expression of sense and antisense insulin-like growth factor (IGF)-binding protein-4 complementary DNA alters the mitogenic response of a human colon cancer cell line (HT-29) by mechanisms that are independent of and dependent upon IGF-I. Cancer Res 54:6563–6570.

Singh P and Rubin N (1993). Insulinlike growth factors and binding proteins in colon cancer. Gastroenterology 105:1218–1237.

Solorzano CC, Jung YD, Bucana CD, McConkey DJ, Gallick GE, McMahon G, and Ellis LM (2001). In vivo intracellular signaling as a marker of antiangiogenic activity. Cancer Res 61:7048–7051.

Takahashi Y, Bucana CD, Cleary KR, and Ellis LM (1998). p53, vessel count, and vascular endothelial growth factor expression in human colon cancer. Int J Cancer 79:34–38.

Takahashi Y, Kitadai Y, Bucana CD, Cleary KR, and Ellis LM (1995). Expression of vascular endothelial growth factor and its receptor, KDR, correlates with vascularity, metastasis, and proliferation of human colon cancer. Cancer Res 55:3964–3968.

Warren RS, Yuan H, Matli MR, Ferrara N, and Donner DB (1996). Induction of vascular endothelial growth factor by insulin-like growth factor 1 in colorectal carcinoma. J Biol Chem 271:29483–29488.

Weidner N (1995). Intratumor microvessel density as a prognostic factor in cancer [comment]. Am J Pathol 147:9–19.

Werner H and Le Roith D (1997). The insulin-like growth factor-I receptor signaling pathways are important for tumorigenesis and inhibition of apoptosis. Crit Rev Oncog 8:71–92.

Wu Y, Yakar S, Zhao L, Hennighausen L, and LeRoith D (2002). Circulating insulin-like growth factor-I levels regulate colon cancer growth and metastasis. Cancer Res 62:1030–1035.